

Colloidal behavior of goethite nanoparticles modified with humic acid and implications for aquifer reclamation

Original

Colloidal behavior of goethite nanoparticles modified with humic acid and implications for aquifer reclamation / Tiraferri, Alberto; Saldarriaga Hernandez, Laura Andrea; Bianco, Carlo; Tosco, Tiziana Anna Elisabetta; Sethi, Rajandrea. - In: JOURNAL OF NANOPARTICLE RESEARCH. - ISSN 1388-0764. - STAMPA. - 19:art. n. 107(2017). [10.1007/s11051-017-3814-x]

Availability:

This version is available at: 11583/2667004 since: 2017-05-30T09:38:08Z

Publisher:

Springer

Published

DOI:10.1007/s11051-017-3814-x

Terms of use:

This article is made available under terms and conditions as specified in the corresponding bibliographic description in the repository

Publisher copyright

(Article begins on next page)



Politecnico di Torino

Colloidal Behavior of Goethite Nanoparticles Modified with Humic Acid and Implications for Aquifer Reclamation

Alberto Tiraferri, Laura Andrea Saldarriaga Hernandez, Carlo Bianco, Tiziana Tosco, Rajandrea Sethi

Original Citation:

A. Tiraferri, L. A. Saldarriaga Hernandez, C. Bianco, T. Tosco, R. Sethi (2017), Colloidal Behavior of Goethite Nanoparticles Modified with Humic Acid and Implications for Aquifer Reclamation. Journal of Nanoparticle Research 19(3), Article number 107, ISSN: 13880764, DOI: 10.1007/s11051-017-3814-x

Availability:

This version is available at: <http://porto.polito.it/2667004/>
since: May 2017

Publisher:
Springer

Published version:

DOI: 10.1007/s11051-017-3814-x

Terms of use:

This article is made available under terms and conditions applicable to Open Access Policy Article ("Public - All rights reserved"), as described at http://porto.polito.it/terms_and_conditions.

(Article begins next page)

Colloidal Behavior of Goethite Nanoparticles Modified with Humic Acid and Implications for Aquifer Reclamation

Alberto Tiraferri, Laura Andrea Saldarriaga Hernandez, Carlo Bianco,
Tiziana Tosco, Rajandrea Sethi *

Journal of Nanoparticle Research 19(3), Art. n. 107

DOI: 10.1007/s11051-017-3814-x

DIATI (Department of Land, Environment and Infrastructure Engineering)

Politecnico di Torino, C.so Duca degli Abruzzi 24, Torino 10129, Italy

* Corresponding Author: phone +39-011-090-7735; fax: +39-011-090-7699; e-mail:

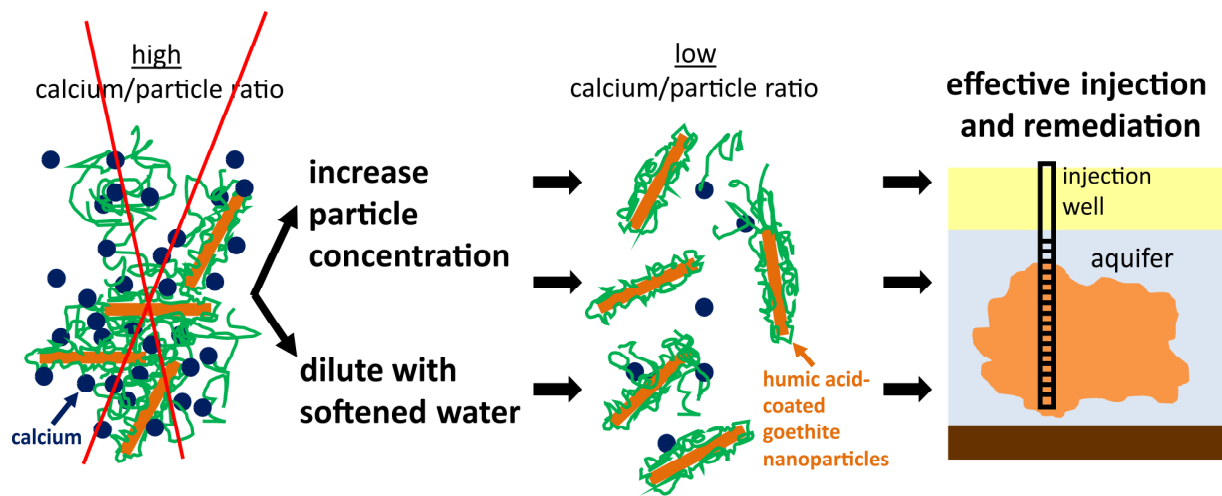
rajandrea.sethi@polito.it

Abstract

Nanosized colloids of iron oxide adsorb heavy metals, enhance the biodegradation of contaminants, and represent a promising technology to clean-up contaminated aquifers. Goethite particles for aquifer reclamation were recently synthesized with a coating of humic acids to reduce aggregation. This study investigates the stability and the mobility in porous media of this material as a function of aqueous chemistry and it identifies the best practices to maximize the efficacy of the related remediation. Humic acid-coated nano-goethite (hydrodynamic diameter ~90 nm) displays high stability in solutions of NaCl, consistent with effective electrosteric stabilization. However, particle aggregation is fast when calcium is present, and to a lesser extent also in the presence of magnesium. This result is rationalized with complexation phenomena related to the interaction of divalent cations with humic acid, inducing rapid flocculation and sedimentation of the suspensions. The calcium dose, i.e., the amount of calcium ions with respect to solids in the dispersion, is the parameter governing stability. Therefore, more concentrated slurries may be more stable and mobile in the subsurface than dispersions of low particle concentration. Particle concentration during field injection should be thus chosen based on concentration and proportion of divalent cations in groundwater.

Keywords: particle stability, site remediation, humic acid, calcium bridging, aggregation, transport, porous media, goethite, calcium dose.

Graphical Abstract



- goethite nanoparticles are used in contaminated site remediation
- the particles are stable in monovalent ion solutions due to an adsorbed layer of humic acids
- above a threshold concentration of divalent cations particles aggregate and sediment
- stability in suspension and transport in porous media correlate well
- high particle/calcium ratios increase stability and facilitate use in field application

1. Introduction

Nanosized iron oxide is a promising material to enhance bioremediation of sites contaminated by organic and inorganic pollutants (Bosch et al. 2010, Lee et al. 2012, Tosco et al. 2012, Braunschweig et al. 2013, Meckenstock and Bosch 2014). Nanoparticles of hematite, ferrihydrite, and goethite have been shown to act as electron acceptors for iron-reducing bacteria during the oxidative degradation of numerous hazardous and recalcitrant compounds (Waychunas et al. 2005, Tobler et al. 2007, Bosch et al. 2010, Braunschweig et al. 2013). They are also effective in the adsorption and immobilization of toxic metals (Benjamin et al. 1996). The high reactivity of these materials is also due to their stability under typical environmental conditions (Keller et al. 2010, Xu et al. 2015), which helps maintaining a large surface area available for reaction. Stability is also a crucial property to optimize the delivery of slurries of iron oxide nanoparticles to directly target the contaminant close to the source of contamination and to create filtration barriers for heavy metals (Tosco et al. 2012, Luna et al. 2015).

The aqueous stability of iron-based and iron oxide nanoparticles is highly influenced by natural or engineered adsorption of polyelectrolytes to their surface (Lowry et al. 2012, Raychoudhury et al. 2012, Philippe and Schaumann 2014, Velimirovic et al. 2014, Tiraferri and Borkovec 2015). The charged chains control the stability of the modified colloids and they can provide long-ranged electrostatic and steric repulsive interactions. The effect of surface coating on particle reactivity has yet to be fully understood, but previous studies suggest that a possible loss in particle reactivity is offset by benefits obtained from reduced aggregation and improved mobility in porous media (Gastone et al. 2014, Velimirovic et al. 2014, Vindedahl et al. 2016, Vindedahl et al. 2016). Furthermore, the organic content at the particle surface was shown to reduce the toxicity of the oxide colloids towards nematodes

(Hoss et al. 2015). Therefore, iron oxide nanoparticles for site remediation have been recently synthesized with a coating of humic acids that form a stabilizing layer on the solid surface.

Humic acids are polyelectrolytes with a high density of carboxylic and phenolic functional groups. While humic substances and humic acids often prevent aggregation and increase the transport of numerous colloids and oxide nanoparticles (Illes and Tombacz 2006, Baalousha 2009, Domingos et al. 2009, Dong and Lo 2013, Chekli et al. 2014, Vindedahl et al. 2016), they are also known to interact strongly with calcium and other metal ions primarily through carboxyl moieties (Hering and Morel 1988, Sander et al. 2004). In fact, accelerated aggregation and deposition have been observed in both natural and engineered systems comprising humic acid and calcium (Dong and Lo 2013). This mechanism may be important during the delivery of nanosized oxides coated with humic acids or other carboxyl-rich polyelectrolytes.

Therefore, a number of practical considerations should be taken into account when designing a remediation based on this technology. The reactive suspensions are produced and delivered at very high concentrations of solids, in the order of 100 g/L. Prior to injection, the concentrated stock is diluted to facilitate handling and this procedure must consider the possible influence of the water chemistry used to treat the dispersion. Once injected in the subsoil, the nanoparticle slurry is then further diluted by groundwater, whose composition needs full characterization. Knowledge of the possible interactions of the nanomaterials undergoing these dilutions with ions present in water is crucial to predict the success of the remediation process (Bianco et al. 2016). In principles, this understanding would allow to specifically design the initial suspension and the various handling steps to achieve the best results for each specific site.

In this study, we evaluate the aqueous behavior of concentrated suspensions of humic acid-coated goethite nanoparticles, recently designed and manufactured for use in reclamation

of contaminated aquifers. We present results obtained at near neutral pH, relevant for groundwater application, and in solutions of NaCl, CaCl₂, MgCl₂, as well as in tap water. In particular, we investigate numerous combinations of dispersed solid content and of ionic composition. We measure the surface potential of the modified nanoparticles and we relate this parameter to their aggregation and to their ability to remain in suspension. We also conduct transport tests in an idealized sandy system, to correlate colloid stability with mobility. Therefore, we identify the main drivers controlling the behavior of suspensions in water and we suggest how to avoid pitfalls and how to maximize the delivery of these nanoparticles to achieve effective site reclamation.

2. Materials and Methods

2.1 Preparation and chemical properties of particle suspensions.

A stock suspension of stable, colloidal goethite nanoparticles with a solid concentration of roughly 110 g/L was obtained from University of Duisburg-Essen (Germany) where it was produced, specifically for site remediation, according to US patent 8,921,091 B2 (Meckenstock and Bosch 2014). During synthesis, the nanoparticles were coated by humic acids, which were added in excess and thus were present in the final suspension both as unadsorbed chains and as adsorbed layers on particles. Large amounts of surface modifiers are needed to functionalize the highly concentrated slurries injected in the subsoil. Among the suitable polymeric modifiers, humic acids were chosen because inexpensive, easy to find and to use, biocompatible, and able to provide the necessary functionalities. Furthermore, humic acids are naturally present in aquifers and would adsorb on the particles once dispersed in groundwater. Unless otherwise stated, the stock suspension was diluted with deionized (DI) water to perform experiments at different values of solid concentration, and the ionic composition of the final suspensions was changed by addition of NaCl, CaCl₂, or MgCl₂.

Some experiments were conducted by diluting the stock suspension in tap water to understand the effect of dilution in field application and they are discussed in the last chapter of this manuscript. According to our inductively coupled plasma, ionic chromatography, and alkalinity analyses, tap water contained 0.3 mM sodium, 2.1 mM calcium, 0.5 mM magnesium, 0.5 mM chloride, 0.4 mM nitrate, 3.6 mM bicarbonate, 0.4 mM sulfate, and other ions at negligible concentrations, yielding a total ionic strength of approximately 11 mM and a total hardness of 260 mg/L as equivalent CaCO_3 . The pH of all suspensions was always stable and between 7.5 and 8, relevant for groundwater application, obtained without addition of a buffer. Experiments were performed at different pH values by addition of small amounts of concentrated HCl or NaOH to the final suspensions. Throughout the text, we refer to the solid or to the slurry content as the concentration of particles plus humic acids in the final suspensions. Both adsorbed and dissolved humic acids contribute to system behavior and are included in the calculations.

2.2 Measurements of size, aggregation rate, and electrophoretic mobility.

Electrophoretic mobility of the humic acid-coated goethite particles was measured over a range of pH values and ionic compositions. The influence of solid concentration was also investigated. The instrument was a ZetaSizer Nano ZSP (Malvern) comprising as light source a He/Ne laser operating at 633 nm. The suspensions were equilibrated for at least 1 min prior to measurement. Several runs were performed for each sample, and the resulting values of electrophoretic mobility were averaged. Zeta potentials were calculated from average electrophoretic mobility values using Smoluchowski equation, assuming that the Debye length of the particle double layer, $1/\kappa$, was always much smaller than the particle radius, a , that is, $\kappa \cdot a \gg 1$ (Elimelech et al. 1995). The same instrument was utilized to measure the kinetics of change in particle size upon variation of the solution chemistry. Suspensions were

initially introduced into a plastic cuvette having 10 mm path length and the hydrodynamic diameter of primary nanoparticles was obtained (initial Z-average, Z_{ave}^0 , of 98 ± 4 nm). Subsequently, an electrolyte at known concentration was introduced into the vial to induce aggregation. Measurements were started immediately after mixing of the suspension. The tests were conducted in backscattering mode at an angle of 173° , with automatic settings. Calculations were carried out by analyzing the change of Z-average values provided by the software, Z_{ave} . Its apparent rate of change was divided by the initial size value and by the solid (particle and humic acids) concentration of each sample, c_S , as $\Sigma = \frac{1}{c_S \cdot Z_{ave}^0} \frac{dZ_{ave}}{dt}$ (units: $\frac{1}{s} \frac{1}{(g/L)}$), proportional to the absolute aggregation rate coefficient, k . The stability ratio was calculated as the apparent rate under conditions of diffusion-limited aggregation regime, divided by the prevailing rate under each investigated condition, $W = \frac{\Sigma|_{fast}}{\Sigma}$, which is thus equivalent to $\frac{k_{fast}}{k}$ (Elimelech et al. 1995, Holthoff et al. 1997). Experiments in diffusion-limited regime were conducted at solid concentrations of 0.22 or 0.11 g/L.

2.3 Batch sedimentation and transport experiments.

For batch sedimentation experiments, dispersions were prepared using the same protocol as for light scattering experiments. The same disposable cuvette with a path length of 10 mm were used, which were filled with 4 mL of suspension and shaken prior to the experiment upon addition of the salt to induce sedimentation. The sedimentation profiles were obtained by measuring the optical density as a function of time at a wavelength of 800 nm using a UV-vis spectrophotometer (Specord S600, Analytik Jena, Germany).

Further batch sedimentation experiments were conducted with suspensions prepared by removing some of the unadsorbed portion of humic acids, thus leaving mostly that adsorbed on the surface of nanoparticles. To this purpose, the stock slurry was filtered in an ultrafiltration setup at low applied pressure (~ 30 psi) using polysulfone membranes with a molecular weight cutoff of approximately 40 nm (PS20, Sepro Membranes, Oceanside, CA). The pore size of the membranes ensured all particles to be retained in the feed solution while letting dissolved polyelectrolytes pass into the permeate, which was discarded. The feed suspension was filtered and re-diluted using DI water in a number of cycles to reduce the amount of non-adsorbed humic acid to a minimum.

Transport experiments were performed in a porous medium consisting of idealized sand (Dorsilit n.7, Dorfner, Germany) with a mean diameter of roughly 0.87 mm. For each test, a chromatographic column with an inner diameter of 16 mm was wet packed with a fixed amount sand (36.5 g dry weight), to achieve an average column length of 11.3 cm. Prior to packing of the column, the sand was cleaned, degassed, and completely hydrated. Porous medium parameters were determined via inverse fitting of breakthrough curves of NaCl used as a conservative tracer, resulting in an average effective porosity of 0.45 and an average dispersivity 6.17×10^{-4} m. The concentration of both salt and colloidal particles at the inlet and outlet of the column was monitored online via optical density measurements in the same spectrophotometer employed for sedimentation experiments, but equipped with flow-through cells characterized by a 2 or 5 mm light path (Hellma, Germany). Monitoring wavelengths of 198.5 nm for NaCl and 800 nm for the colloids were chosen: linear relationship between absorbance and concentration was observed at these wavelengths. To conduct the transport test, the column was equilibrated by flushing it with DI water, followed by five pore volumes of solution at the same background ionic composition used later for particle injection. Then, the experiments included the injection of five pore volumes of the slurry, followed by

flushing of the column with five more pore volumes of the particle-free background solution. Further details on the setup are given in previous publications (Tosco et al. 2012).

3. Results and Discussion

3.1 The dose of calcium governs the behavior of concentrated nanoparticle slurries.

Humic acids adsorb onto oxide particles, determining their surface properties (Lowry et al. 2012, Philippe and Schaumann 2014, Tiraferri and Borkovec 2015). The goethite nanoparticles investigated in this study had a saturated coating of humic acid (Maroni et al. 2015). The surface potential of modified goethite particles was thus governed by the behavior of the adsorbed polyelectrolyte chains, as illustrated in Figure 1 (Szilagyi et al. 2014).

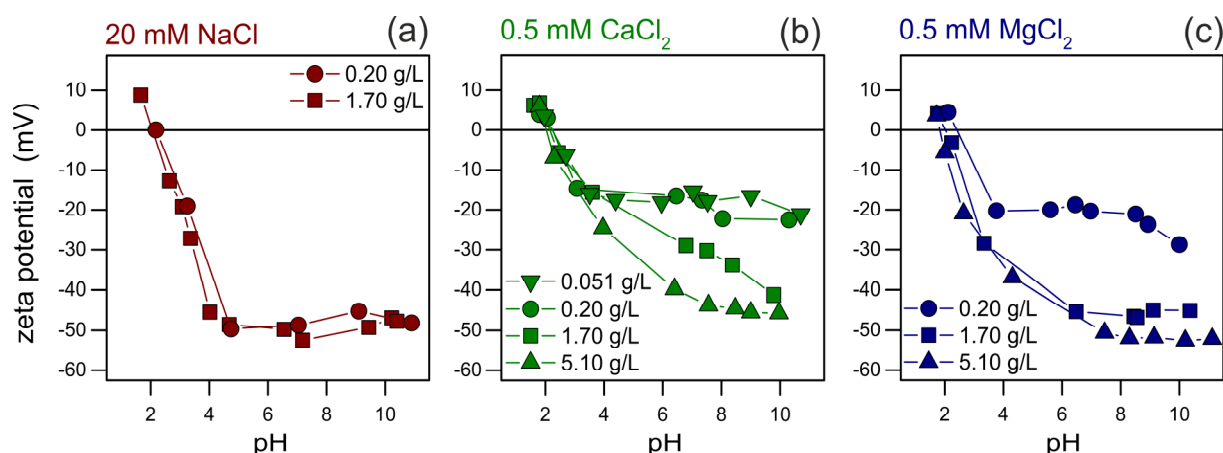


Fig. 1 Zeta potential of humic acid-coated goethite nanoparticle suspensions as a function of pH in (a) 20 mM NaCl, (b) 0.5 mM CaCl_2 , and (c) 0.5 mM MgCl_2 . Zeta potentials were calculated using Smoluchowski equation from electrophoretic mobility values, measured at varying slurry concentrations. Data points are averages of at least three runs; lines are intended to be used as guide for the eyes only. Experiments were performed at 25°C

The isoelectric point of the suspensions was approximately 3 in all cases, consistently with charging of carboxylic groups of humic acid. Above this pH, nanoparticles exhibited negative values of zeta potential. While the potential reached a plateau at roughly -50 mV in

NaCl solution regardless of slurry concentration, in the presence of calcium and magnesium counterions, the charging behavior was influenced by the amount of solids in suspension. In particular, slurries of lower particle concentration exhibited values of zeta potential of lower magnitude. Similar results were observed when mobilities were measured at a fixed pH of 7.5-8 and as a function of ionic strength; see Figure S1 of Online Resource 1. This result is rationalized with complexation of counterions with humic acid adsorbed on the nanoparticle surface. Divalent cations may also form complexes with the goethite surface, thus further influencing the electrophoretic mobility. As the slurry concentration decreased, the density of complexed ions increased, causing a reduction of the overall negative potential.

This mechanism is better illustrated in Figure 2, where values of zeta potential are plotted as a function of dose. Dose is here defined as the ratio between the mass of added counterion in solution and the mass of solids in suspension. The latter parameter was used as a proxy for the amount of functional groups in the system, based on the assumptions that their concentration is proportional to solid content. Therefore, Figure 2 provides a semi-quantitative description of the change of zeta potential due to the interaction of ions in solution with functional groups adsorbed on particle surface.

Plots in Figure 2 suggest that the zeta potential of nanoparticle slurries depended on the dose of counterion and not merely on solid or ion concentration, as the data points measured at different dilutions but at the same ion dose overlap nicely. The steep decrease of potential values at around 0.01 calcium dose and 0.03 magnesium dose suggests that a threshold concentration of divalent cations exist, above which suspensions become rapidly unstable. The higher amount of magnesium needed to cause this change imply higher ability of calcium to form complexes with the functional groups in the system. No change in zeta potential was observed at relatively low concentrations of NaCl, suggesting weak specific interactions of sodium with goethite and with humic acids.

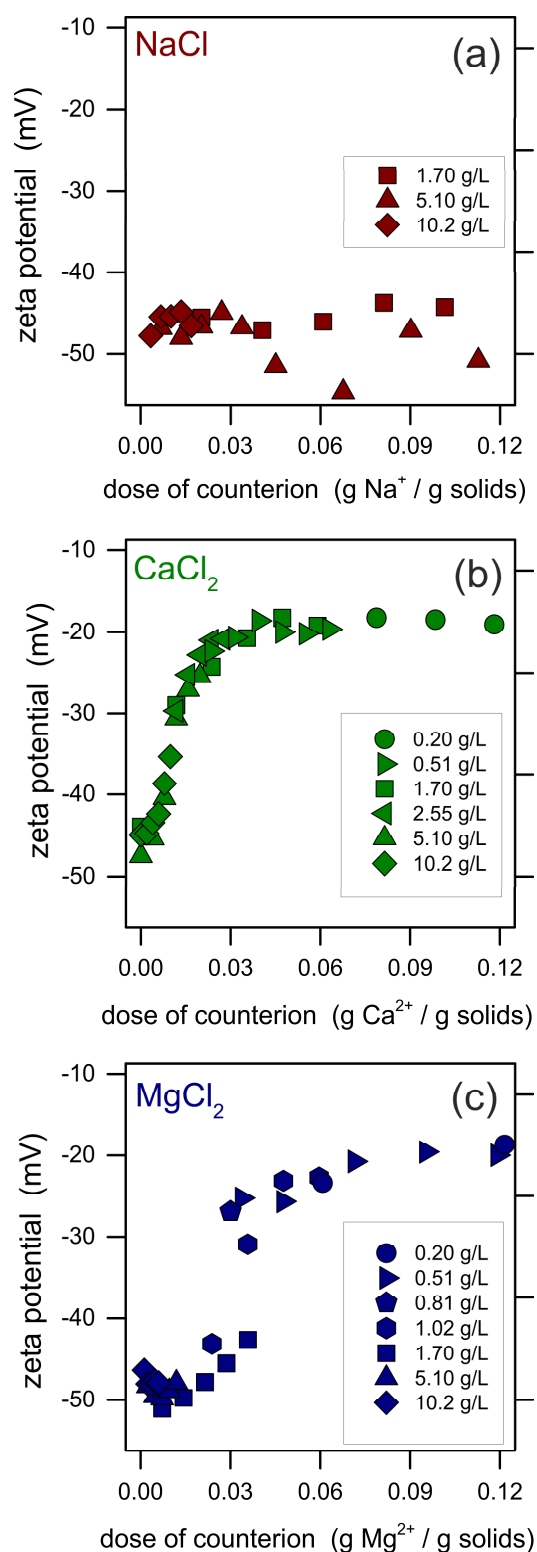


Fig. 2 Zeta potential of humic acid-coated goethite nanoparticle suspensions as a function of dose of (a) NaCl, (b) CaCl₂, and (c) MgCl₂. Zeta potentials were calculated using Smoluchowski equation from electrophoretic mobility values, measured at varying slurry concentrations and at pH 7.5-8. Data points are averages of at least three runs. Experiments were performed at 25°C

Figure 3a shows the stability ratio as a function of NaCl concentration. The observed trend is typical for colloidal aggregation and it may be explained with DLVO theory. A reaction-limited regime was followed by a diffusion-limited regime to aggregation in increasing salt, whereby probability of aggregation upon collision was highest (Elimelech et al. 1995). High NaCl concentration was needed to destabilize the suspension, which supports the observation that the adsorbed polyelectrolyte had a high charge density (Illes and Tombacz 2006, Domingos et al. 2009). The critical coagulation concentration, CCC, of NaCl was close to 450 mM. It is important to note that the stability ratio was independent of particle concentration in the presence of sodium, as aggregation experiments conducted at different dilutions yielded comparable results. Typical data obtained from aggregation experiments in the presence of NaCl are presented in Figure S2 of Online Resource 1. A different outcome was obtained when calcium was added to induce aggregation. Aggregation behavior was found to depend strongly on slurry concentration. This influence is evident in Figure 3b, where the data points of apparent aggregation rate divided by the solid concentration decrease as this concentration increased, in the same solution containing 1.4 mM CaCl_2 . This decrease is substantial, as a five-fold increase in solid concentration produced a reduction of aggregation rate of roughly four orders of magnitude. These results are consistent with those of electrophoresis experiments: lower solid content in the slurry, i.e., higher calcium doses, was related to particles with lesser negative surface potential that did not allow effective stabilization. However, they are also somewhat counterintuitive, as they imply that suspensions of larger particle concentrations are significantly more stable than their diluted counterparts. An analogous trend was observed upon addition of 0.7 mM CaCl_2 ; see Figure S3 of Online Resource 1. The aggregation behavior with calcium cannot be explained by DLVO theory and we suspect that attractive bridging interactions induced by calcium counterions might be significant in this system. Bridging occurs through the formation of

complexes between calcium ions and the carboxyl functional groups on humic acid chains adsorbed on different nanoparticles (Sander et al. 2004, Chen et al. 2007).

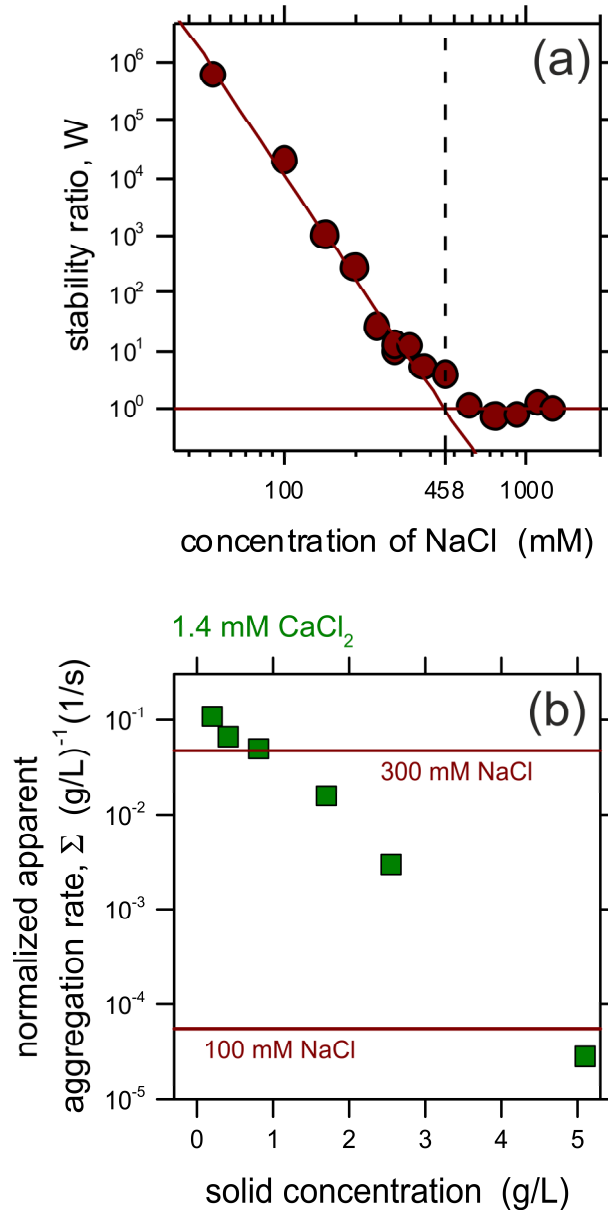


Fig. 3 Results of aggregation experiments. (a) Stability ratio as a function of NaCl concentration (red circles). Continuous lines represent the best fits of the stability ratio in the reaction-limited regime and in the diffusion-limited regime. The CCC occurring at their intersection is indicated by a vertical dashed line. (b) Apparent aggregation rate (green squares), $\Sigma = \frac{1}{c_s \cdot Z_{ave}^0} \frac{dZ_{ave}}{dt}$, as a function of slurry concentration in the presence of 1.4 mM CaCl_2 . For comparison, two horizontal lines are added to this second plot to represent the normalized rate, independent of solid concentration, which would be observed in 100 mM NaCl and 300 mM NaCl. Experiments were conducted at 25°C and at a pH value of 7.5

3.2 There is a threshold concentration of calcium above which suspensions are unstable.

Sedimentation and transport of goethite nanoparticle dispersions were studied to evaluate how the influence of aqueous chemistry, discussed above, may translate into efficacy of delivery into the subsurface. Figure 4a shows data of exemplificative batch sedimentation tests carried out at fixed slurry content and by varying the concentration of CaCl_2 . Table S1 of Online Resource 1 presents pictures of the vials related to these tests. Experiments conducted with MgCl_2 and with different amounts of solids in suspension are also summarized in Online Resource 1 (Figure S4). As the concentration of divalent cations increased, aggregation and sedimentation became faster. Low concentrations of calcium (between 0.5 and 2.0 mM, equivalent to hardness of 50 to 200 mg/L expressed as CaCO_3) were needed to induce sedimentation of the dispersions investigated here within a few hours. At the same slurry concentrations, higher amount of magnesium was required to produce sedimentation, consistently with zeta potential results presented above. We underline that the settling conditions in our experiments were far from a regime of compression sedimentation and that sedimentation results correlated well with the hydrodynamic size of particles measured for some of the samples at the end of the batch settling test.

During field works for particle injection, slurries of modified goethite nanoparticles need to remain in suspension for several hours. From the sedimentation tests carried out at each different particle content, we confirmed the hypothesis that there is a threshold concentration of calcium above which this ion is capable to induce destabilization of the suspensions. In particular, we identified the threshold calcium concentration causing sedimentation of each suspension in less than five hours. We chose this time frame based on a purely empirical rationale based on the typical time needed to maintain slurries stable during field injection. Just as an example, the threshold calcium concentration for the data plotted in Figure 4a would be 1 mM. We then graphed these values of threshold counterion concentration as a

function of related slurry content in Figure 4b. The obtained trend is nearly linear and the slope value may be directly used to design a remediation activity, when the calcium content in groundwater is known. Below (lower calcium concentration) or to the right (larger solid concentration) of this line, the system is stable because the calcium dose is below the destabilization threshold, and vice versa.

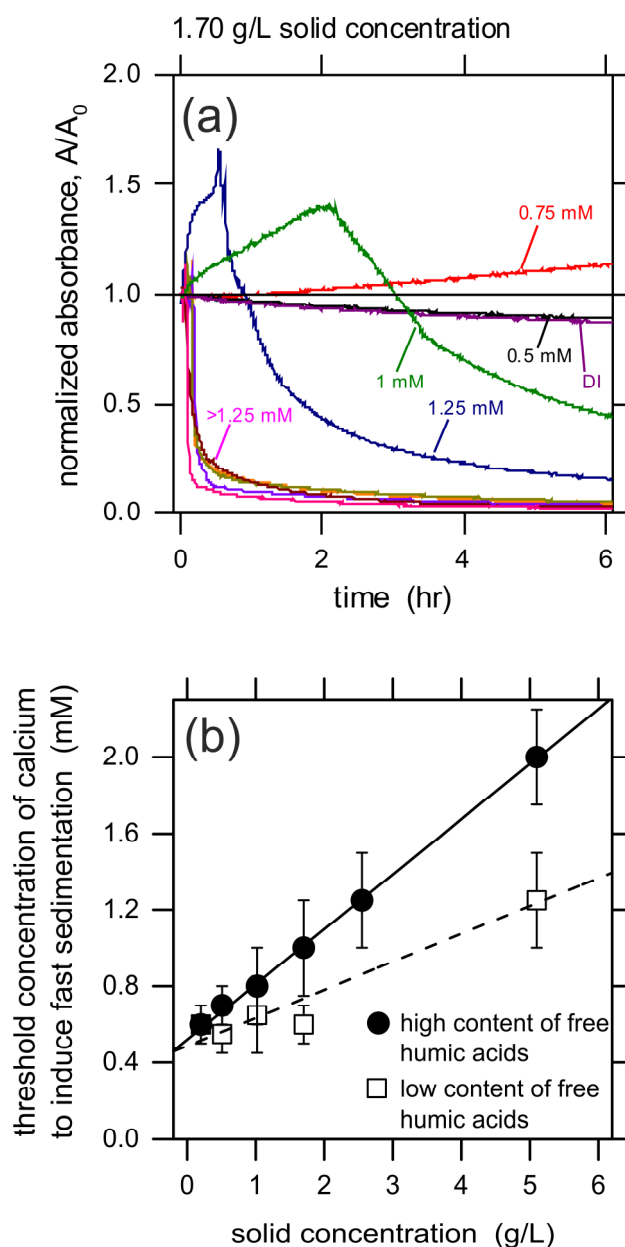


Fig. 4 Results of sedimentation experiments. (a) Normalized light absorbance of samples at 800 nm wavelength for a solid content of 1.70 g/L and varying concentration of CaCl_2 . The different concentrations are labeled. (b) Concentration of calcium needed to induce sedimentation of the nanoparticle suspension within a few hours of sample preparation as a function of solid content. Solid circles refer to experiments conducted with each diluted suspension tested as is, while open squares are data points associated with suspensions from which most of the

dissolved humic acids were removed by filtration. All experiments were performed at pH 7.5-8 and at temperature of 25 °C

Few batch sedimentation tests were performed with suspensions containing lower amount of unadsorbed humic acids, which were removed by filtration. The results obtained with the filtered dispersions are presented as open squares in Figure 4b. When some of the unadsorbed chains of humic acids were removed, the concentration of calcium needed to destabilize the suspension decreased compared to unfiltered suspensions at the same dilution; see sedimentation curves in Figure S5 of Online Resource 1. As expected, the intercept of the best fit line of these data is the same as in the case of unfiltered suspension, but its slope was roughly halved. This observation suggests that dissolved polyelectrolyte chains were responsible for sequestering a portion of calcium ions, rendering these cations unavailable for complexation and for bridging mechanisms. This contribution was not negligible and deserves further investigation. Additionally, the interaction of unadsorbed humic acids with contaminants in the aquifer may be important especially for substances with low polarity and it should also be understood.

3.3 Transport of suspensions in porous media may be enhanced by working at high particle concentration.

Transport experiments conducted under idealized conditions confirmed that mobility is closely related to aqueous stability; see Figure 5 as well as Figures S6 and S7 of Online Resource 1. Nanoparticles were highly mobile in sand saturated with solutions of NaCl, consistent with predictions of colloid filtration theory under unfavorable attachment conditions. Previous studies have also discussed similar transport of iron-based and metal oxide nanoparticles upon modification with acidic polyelectrolytes and organic matter (Petosa et al. 2012, Raychoudhury et al. 2012, Dong and Lo 2013, Tosco et al. 2014, Velimirovic et

al. 2014). It is possible that unadsorbed humic acid chains contributed to the mobility by coating the sand grains and providing an electrosteric barrier to particle deposition.

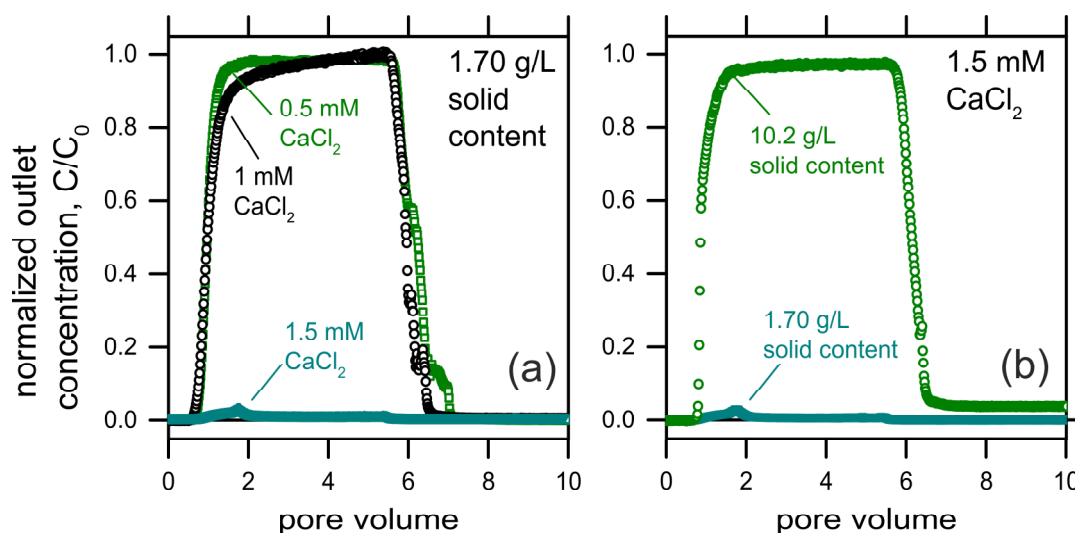


Fig. 5 Breakthrough curves of humic acid-coated goethite nanoparticles in silica sand (a) at 1.70 g/L solid content and in the presence of CaCl₂ at different concentrations and (b) in 1.5 mM CaCl₂ at varying solid content. In the y-axis, the value of concentration at the outlet with respect to the injected concentration, C₀, both calculated from values of light absorbance at 800 nm wavelength based on a calibration line. In the x-axis, the pore volumes injected into the column. The nanoparticle suspension was introduced at time 0. The key experimental conditions were: pH 7.5-8, pore volume 10.2 mL, temperature 25 °C, and approach velocity 1.7×10^{-4} m/s

Figure 5a shows that a suspension of 1.70 g/L slurry content was highly transported in CaCl₂ solutions of 0.5 mM and 1 mM. These concentrations of calcium were in fact equal or lower than the threshold value needed to cause sedimentation of the suspensions in few hours; see Figure 4a. Particles in the inlet tank had a hydrodynamic radius of less than 200 nm under both conditions at the end of the tests. However, a change in calcium concentration to 1.5 mM, above the destabilization threshold, resulted in negligible transport of the dispersion within the sandy column. These results cannot be simply explained by colloid filtration theory and are mostly due to the large aggregates forming within the pores, causing mechanical filtration, physical straining, and ripening effects. Data collected by keeping the same calcium concentration and increasing slurry content to 10.2 g/L show that this new

dispersion of lower dose was again transported easily through the porous medium; see Figure 5b. For this experiment, nanoparticles in the injection tank were stable and had a hydrodynamic diameter of 104 nm at the end of the test, thus preventing filtration phenomena that would have occurred in the presence of aggregates. These results confirm that the transition between stable and unstable suspensions may be relatively sharp and that sedimentation tests may be successfully used also to predict mobility within the subsurface.

3.4 Practical considerations regarding slurry stability in field applications.

Contrary to zerovalent iron particles that are poorly stable due to magnetic attractive forces (Tosco et al. 2014, Luna et al. 2015), the slurries investigated in this study are characterized by strong electrosteric repulsive interactions imparted by humic acids that prevent aggregation and deposition in solutions of monovalent ions. However, the same modification responsible for such stabilization gives rise to phenomena that may cause sedimentation of the suspension in the presence of relatively low concentrations of calcium. When the concentration of the suspension is low, the low amount of carboxyl groups imparting stability may be neutralized and bridged by calcium ions in solution. Therefore, higher particle loads would guarantee that a larger density of ionized carboxyl groups remain available to provide electrostatic repulsion.

All the results discussed so far were observed in solution obtained by adding salts or pH adjusters to deionized water. In the field, dilution of the stock suspension using readily available tap water would simplify the engineering works and would translate into an economic advantage compared to the use of pure water. We have investigated the possible effects of such dilution on the suspension stability by using tap water from our lab at Politecnico di Torino. This water has an average pH of 7.4, it contains approximately 2.1 mM calcium, 0.3 mM sodium, and has a total ionic strength of roughly 11 mM and hardness of

260 mg/L as CaCO_3 . Figure 6 summarizes the results of zeta potential, sedimentation, and transport obtained with these samples at various dilutions. The relatively high concentration of calcium in tap water resulted in reduced values of measured electrophoretic mobility compared to the initial stock. These values were closer to zero as the slurry content in the suspension decreased, consistent with results obtained in synthetic calcium solutions and discussed above; see Figure 6a. Values of zeta potential with absolute magnitude smaller than 30 mV resulted in rapid aggregation and sedimentation of the suspensions obtained by diluting the stock 20 and 60 times, characterized by a final hardness of 247 and 256 mg/L as CaCO_3 , respectively. Data obtained within six hours of sedimentation are presented in Figures 6b and 6d. The most concentrated dispersion (10× dilution, hardness of 234 mg/L as CaCO_3) did not sediment during 24 hours, as summarized in Table S2 of Online Resource 1. Data from transport experiments in Figure 6c and in Table S3 of Online Resource 1 agree well with sedimentation results. The most mobile suspension in sand resulted from the lowest dilution (10× dilution) of the initial stock of nanoparticles. The hydrodynamic diameter of these particles was measured as 126 nm in the injection tank at the end of the experiment, suggesting little aggregation occurring during the test. While a 20× dilution of the dispersion reduced the mobility slightly, it was not possible to evaluate the transport of the more diluted suspensions as they sedimented quickly during injection.

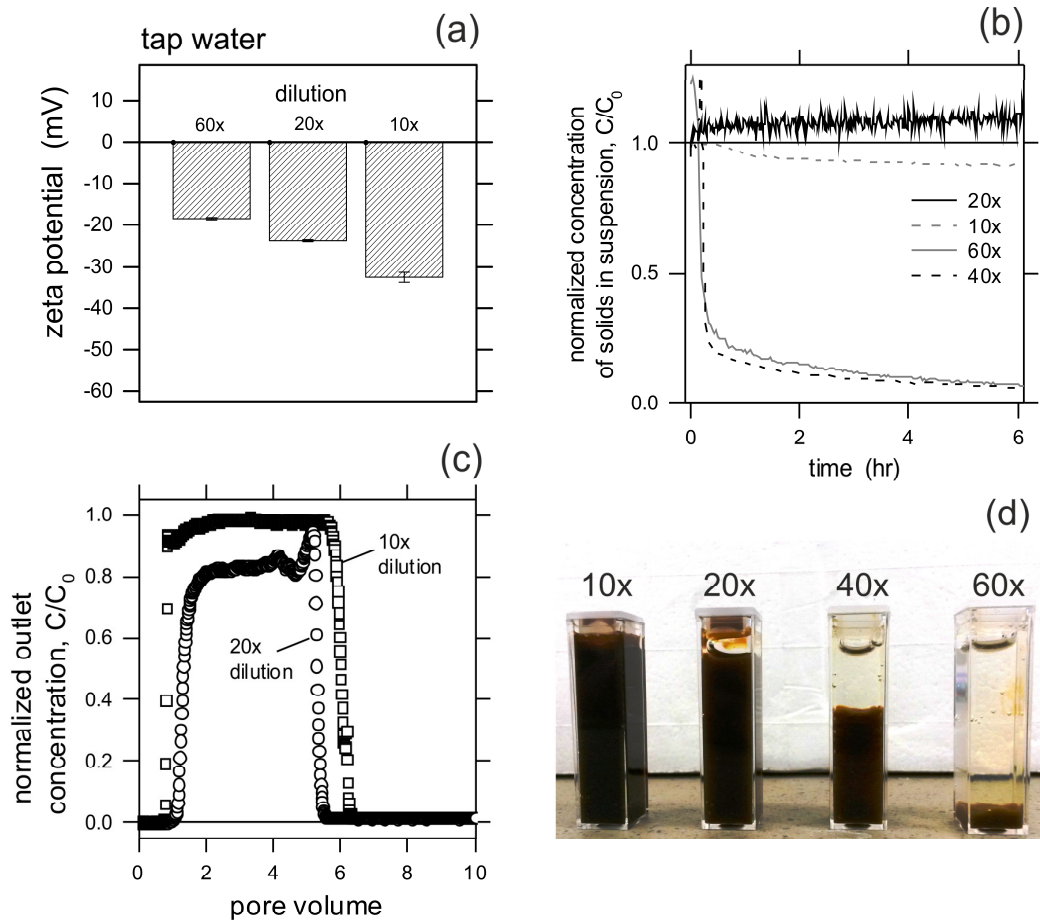


Fig. 6 Behavior of humic acid-coated goethite nanoparticles diluted in tap water from Politecnico di Torino as a function of dilution. (a) Zeta potential, (b,d) sedimentation within six hours, and (c) transport in sandy columns.

All experiments were performed at pH 7.5-8 and temperature of 25°C. Unless specified, all other conditions were analogous to those in previously discussed experiments

4. Conclusions

This manuscript discussed the colloidal stability of goethite particles modified with humic acids as a function of chemistry and ionic composition under near neutral pH conditions. Behavior of these suspensions was dominated by the presence of divalent cations and in particular of calcium. These ions form complexes with both the dissolved and the adsorbed chains of humic acid, thus reducing electrosteric stabilization and giving rise to attractive bridging interactions among particles. The dose of calcium is the most important parameter to be considered when designing particle-driven remediation. At a solid content in the range

of 1-10 g/L, concentrations of about 1-2 mM of calcium are sufficient to cause rapid sedimentation of the suspensions, thus possibly impairing the remediation process.

These results suggest a practice to tune the mobility of the nanoparticle slurries to target specific subsurface areas to be reclaimed. If the aim is to enhance mobility as much as possible, lower extent of dilution of the particle stock would unintuitively represent a better practice. Once injected into the subsurface, suspensions will be naturally diluted by groundwater. As long as the system is below a certain calcium/particle dose, the slurries are mobile in groundwater, while above a certain dose value they deposit, ideally forming reactive zones. During the remediation design stage, we suggest to perform qualitative sedimentation studies in different dilutions obtained by using groundwater from each specific contaminated site. These tests would allow prediction of the suspension mobility in the subsurface and estimation of the approximate particle travel distance.

Electronic Supplementary Material (submitted separately)

Electrophoretic mobility of humic acid-coated goethite nanoparticle suspensions as a function of ionic strength. Examples of raw data from aggregation experiments. Apparent aggregation rate as a function of slurry concentration in the presence of 0.7 mM CaCl_2 . Additional results of sedimentation experiments at varying concentration of CaCl_2 and MgCl_2 . Pictures of sedimentation vials for different doses of calcium. Representative results of sedimentation experiments of suspensions from which most of the unadsorbed humic acid were removed by filtration. Breakthrough curves of humic acid-coated goethite nanoparticles (total solid content of 1.70 g/L) in silica sand in 10 mM NaCl. Pictures of the column during transport tests carried out in 1.5 mM CaCl_2 and 10 g/L solid content. Pictures of sedimentation vials for different dilutions in tap water. Results of transport tests conducted with suspensions diluted with tap water (PDF).

Acknowledgments

This work was partly funded by H2020 EU project ‘Reground’, G.A. n. 641768. We are grateful to Dr. Rainer Meckenstock (University of Duisburg-Essen, Germany) for providing the goethite particles stock suspension. We thank Fabrizio Bianco and Dr. Adriano Fiorucci (Politecnico di Torino) for chemical analyses on tap water.

References

- Baalousha, M. (2009). Aggregation and disaggregation of iron oxide nanoparticles: Influence of particle concentration, pH and natural organic matter. *Sci Total Environ* 407(6):2093-2101, DOI 10.1016/j.scitotenv.2008.11.022
- Benjamin, M. M., R. S. Sletten, R. P. Bailey and T. Bennett (1996). Sorption and filtration of metals using iron-oxide-coated sand. *Water Res* 30(11):2609-2620, DOI 10.1016/S0043-1354(96)00161-3
- Bianco, C., T. Tosco and R. Sethi (2016). A 3-dimensional micro-and nanoparticle transport and filtration model (MNM3D) applied to the migration of carbon-based nanomaterials in porous media. *J Contam Hydrol* 193:10-20, 10.1016/j.jconhyd.2016.08.006
- Bosch, J., K. Heister, T. Hofmann and R. U. Meckenstock (2010). Nanosized Iron Oxide Colloids Strongly Enhance Microbial Iron Reduction. *Appl Environ Microb* 76(1):184-189, DOI 10.1128/Aem.00417-09
- Braunschweig, J., J. Bosch and R. U. Meckenstock (2013). Iron oxide nanoparticles in geomicrobiology: from biogeochemistry to bioremediation. *New Biotechnol* 30(6):793-802, DOI 10.1016/j.nbt.2013.03.008
- Cekli, L., S. Phuntsho, L. D. Tijing, J. L. Zhou, J. H. Kim and H. K. Shon (2014). Stability of Fe-oxide nanoparticles coated with natural organic matter under relevant environmental conditions. *Water Sci Technol* 70(12):2040-2046, DOI 10.2166/wst.2014.454
- Chen, K. L., S. E. Mylon and M. Elimelech (2007). Enhanced aggregation of alginate-coated iron oxide (hematite) nanoparticles in the presence of, calcium, strontium and barium cations. *Langmuir* 23(11):5920-5928, DOI 10.1021/la063744k
- Domingos, R. F., N. Tufenkji and K. J. Wilkinson (2009). Aggregation of titanium dioxide nanoparticles: Role of a fulvic acid. *Environ Sci Technol* 43(5):1282-1286, DOI 10.1021/es8023594
- Dong, H. R. and I. M. C. Lo (2013). Influence of calcium ions on the colloidal stability of surface-modified nano zero-valent iron in the absence or presence of humic acid. *Water Res* 47(7):2489-2496, DOI 10.1016/j.watres.2013.02.022
- Dong, H. R. and I. M. C. Lo (2013). Influence of humic acid on the colloidal stability of surface-modified nano zero-valent iron. *Water Res* 47(1):419-427, DOI 10.1016/j.watres.2012.10.013
- Elimelech, M., J. Gregory, X. Jia and R. A. Williams (1995). Particle deposition and aggregation: Measurement, modeling, and simulation. Oxford, Butterworth-Heinemann Ltd.
- Gastone, F., T. Tosco and R. Sethi (2014). Guar gum solutions for improved delivery of iron particles in porous media (Part 1): Porous medium rheology and guar gum-induced clogging. *J Contam Hydrol* 166:23-33, 10.1016/j.jconhyd.2014.06.013
- Hering, J. G. and F. M. M. Morel (1988). Humic-Acid Complexation of Calcium and Copper. *Environ Sci Technol* 22(10):1234-1237, DOI 10.1021/Es00175a018
- Holthoff, H., A. Schmitt, A. FernandezBarbero, M. Borkovec, M. A. CabrerizoVilchez, P. Schurtenberger and R. HidalgoAlvarez (1997). Measurement of absolute coagulation rate constants for colloidal particles: Comparison of single and multiparticle light scattering techniques. *J Colloid Interface Sci* 192(2):463-470, DOI 10.1006/jcis.1997.5022

- Hoss, S., A. Fritzsche, C. Meyer, J. Bosch, R. U. Meckenstock and K. U. Totsche (2015). Size- and Composition-Dependent Toxicity of Synthetic and Soil-Derived Fe Oxide Colloids for the Nematode *Caenorhabditis elegans*. *Environ Sci Technol* 49(1):544-552, DOI 10.1021/es503559n
- Illes, E. and E. Tombacz (2006). The effect of humic acid adsorption on pH-dependent surface charging and aggregation of magnetite nanoparticles. *J Colloid Interface Sci* 295(1):115-123, DOI 10.1016/j.jcis.2005.08.003
- Keller, A. A., H. T. Wang, D. X. Zhou, H. S. Lenihan, G. Cherr, B. J. Cardinale, R. Miller and Z. X. Ji (2010). Stability and aggregation of metal oxide nanoparticles in natural aqueous matrices. *Environ Sci Technol* 44(6):1962-1967, DOI 10.1021/es902987d
- Lee, K. Y., J. Bosch and R. U. Meckenstock (2012). Use of metal-reducing bacteria for bioremediation of soil contaminated with mixed organic and inorganic pollutants. *Environ Geochem Hlth* 34:135-142, DOI 10.1007/s10653-011-9406-2
- Lowry, G. V., K. B. Gregory, S. C. Apte and J. R. Lead (2012). Transformations of nanomaterials in the environment. *Environ Sci Technol* 46(13):6893-6899, DOI 10.1021/Es300839e
- Luna, M., F. Gastone, T. Tosco, R. Sethi, M. Velimirovic, J. Gemoets, R. Muysshondt, H. Sapon, N. Klaas and L. Bastiaens (2015). Pressure-controlled injection of guar gum stabilized microscale zerovalent iron for groundwater remediation. *J Contam Hydrol* 181:46-58, DOI 10.1016/j.jconhyd.2015.04.007
- Maroni, P., F. J. M. Ruiz-Cabello, C. Cardoso and A. Tiraferri (2015). Adsorbed Mass of Polymers on Self-Assembled Mono layers: Effect of Surface Chemistry and Polymer Charge. *Langmuir* 31(22):6045-6054, DOI 10.1021/acs.langmuir.5b01103
- Meckenstock, R. U. and J. Bosch (2014). Method for the degradation of pollutants in water and/or soil. United States. **US8921091 B2**.
- Petosa, A. R., S. J. Brennan, F. Rajput and N. Tufenkji (2012). Transport of two metal oxide nanoparticles in saturated granular porous media: Role of water chemistry and particle coating. *Water Res* 46(4):1273-1285, DOI 10.1016/j.watres.2011.12.033
- Philippe, A. and G. E. Schaumann (2014). Interactions of dissolved organic matter with natural and engineered inorganic colloids: A review. *Environ Sci Technol* 48(16):8946-8962, DOI 10.1021/Es502342r
- Raychoudhury, T., N. Tufenkji and S. Ghoshal (2012). Aggregation and deposition kinetics of carboxymethyl cellulose-modified zero-valent iron nanoparticles in porous media. *Water Res* 46(6):1735-1744, DOI 10.1016/j.watres.2011.12.045
- Sander, S., L. M. Mosley and K. A. Hunter (2004). Investigation of interparticle forces in natural waters: Effects of adsorbed humic acids on iron oxide and alumina surface properties. *Environ Sci Technol* 38(18):4791-4796, DOI 10.1021/es049602z
- Szilagyi, I., G. Trefalt, A. Tiraferri, P. Maroni and M. Borkovec (2014). Polyelectrolyte adsorption, interparticle forces, and colloidal aggregation *Soft Matter* 10:2479-2502, DOI 10.1039/C3SM52132J
- Tiraferri, A. and M. Borkovec (2015). Probing effects of polymer adsorption in colloidal particle suspensions by light scattering as relevant for the aquatic environment: An overview. *Sci Total Environ* 535:131-140, DOI 10.1016/j.scitotenv.2014.11.063

- Tobler, N. B., T. B. Hofstetter, K. L. Straub, D. Fontana and R. P. Schwarzenbach (2007). Iron-mediated microbial oxidation and abiotic reduction of organic contaminants under anoxic conditions. *Environ Sci Technol* 41(22):7765-7772, DOI 10.1021/Es071128k
- Tosco, T., J. Bosch, R. U. Meckenstock and R. Sethi (2012). Transport of Ferrihydrite Nanoparticles in Saturated Porous Media: Role of Ionic Strength and Flow Rate. *Environ Sci Technol* 46(7):4008-4015, DOI 10.1021/es202643c
- Tosco, T., F. Gastone and R. Sethi (2014). Guar gum solutions for improved delivery of iron particles in porous media (Part 2): Iron transport tests and modeling in radial geometry. *J Contam Hydrol* 166:34-51, DOI 10.1016/j.jconhyd.2014.06.014
- Tosco, T., M. P. Papini, C. C. Viggi and R. Sethi (2014). Nanoscale zerovalent iron particles for groundwater remediation: a review. *J Clean Prod* 77:10-21, DOI 10.1016/j.jclepro.2013.12.026
- Velimirovic, M., Q. Simons and L. Bastiaens (2014). Guar gum coupled microscale ZVI for in situ treatment of CAHs: Continuous-flow column study. *J Hazard Mater* 265:20-29, DOI 10.1016/j.jhazmat.2013.11.020
- Vindedahl, A. M., M. S. Stemig, W. A. Arnold and R. L. Penn (2016). Character of Humic Substances as a Predictor for Goethite Nanoparticle Reactivity and Aggregation. *Environ Sci Technol* 50(3):1200-1208, DOI 10.1021/acs.est.5b04136
- Vindedahl, A. M., J. H. Strehlau, W. A. Arnold and R. Lee Penn (2016). Organic matter and iron oxide nanoparticles: aggregation, interactions, and reactivity. *Environmental Science: Nano* 3:494-505, DOI 10.1039/C5EN00215J
- Waychunas, G. A., C. S. Kim and J. F. Banfield (2005). Nanoparticulate iron oxide minerals in soils and sediments: unique properties and contaminant scavenging mechanisms. *J Nanopart Res* 7(4-5):409-433, DOI 10.1007/s11051-005-6931-x
- Xu, C. Y., K. Y. Deng, J. Y. Li and R. K. Xu (2015). Impact of environmental conditions on aggregation kinetics of hematite and goethite nanoparticles. *J Nanopart Res* 17(10: 394):1-14, DOI 10.1007/S11051-015-3198-8